Mol. Cryst. Liq. Cryst., Vol. 531: pp. 40/[340]–46/[346], 2010

ISSN: 1542-1406 print/1563-5287 online
DOI: 10.1080/15421406.2010.499313

Synthesis and Characterization of Bis-Orthometalated Ir(III) Complex Consisting of Non-Carbon-Coordinating Ligand

CHANG-LYOUL LEE,[1,†] RUPASREE RAGINI DAS,[2,†] AND JANG-JOO KIM[3]

[1]Advanced Photonics Research Institute, Gwangju Institute of Science and Technology, Gwangju, Korea
[2]Samsung Advanced Institute of Technology, Yongin, Korea
[3]School of Materials Science and Engineering, Center for Organic Light Emitting Diode, Seoul National University, Seoul, Korea

We have synthesized a new green emitting bis-orthometalated Ir(III) complex, Ir(mpz)$_2$hbz, (where mpz is 3-methyl-1-phenyl pyrazole and hbz is the anion of 2′-hydroxy-2-phenylbenzoxazole) and investigated the device performance by doping it in a mixture of PVN (poly-vinylnapthalene) (60 wt%) and PBD (2-(4-tert-butylphenyl)-5-(4-biphenylyl)-1,3,4-oxadiazole) (40 wt%) or PVK (poly-vinylcarbazole) with 8 wt% doping concentration. The Ir(mpz)$_2$hbz doped PVN:PBD device demonstrates a better device performance than that of Ir(mpz)$_2$hbz doped PVK device due to better hole and electron balance in the emissive layer. The maximum external quantum efficiency (η_{ext}) of 8 wt% Ir(mpz)$_2$hbz doped PVN:PBD device is ~1.2% at 12 mA/cm^2. The maximum brightness is 5,800 cd/m^2 at 18 V. This work shows that phosphorescent Ir(III) complex which emits the luminescence from the MLCT transition based on a non-carbon-coordinating ligand can comply with the device demand.

Keywords Bis-orthometalated Ir(III) complex; light-emitting diode; non-carbon-coordinating ligand; PVK

Introduction

The ligand variation in transition metal complexes can tune its photophysical properties as well as influence device performances. The Ir(III) complexes which are used in polymer (organic) electrophosphorescent LEDs usually emit from an admixture of ^{3}MLCT (triplet metal-to-ligand charge-transfer) and ligand centered π-π^* state [1] for efficient phosphorescent emission. But, certain ligands split *d*-orbitals to such an extent that the energy gap between the metal *d*-orbital and the ligand-π^* orbital lies above the visible range [2]. Therefore, the emission takes place

---

[†] These authors contributed equally to this work.

Address correspondence to Dr. Chang-Lyoul Lee, Advanced Photonics Research Institute, Gwangju Institute of Science and Technology, Gwangju, 500-712, Korea. Tel.: (+82)62-715-3347; Fax: (+82)62-715-3360; E-mail: vsepr@gist.ac.kr

near the UV region and it is considerably weak as the high lying emitting state which is close to other excited states of higher energies, causing a resonance between the emitting and higher states. In such a case, the presence of another ligand of weaker ligand field strength can cause efficient emission from a low-lying MLCT state. In this paper, a new green emitting Ir(III) complex, Ir(mpz)$_2$hbz, (mpz is 3-methyl-1-phenyl pyrazole and hbz is the anion of 2′-hydroxy-2-phenylbenzoxazole) has been synthesized and characterized. It emits luminescence from the MLCT state based on non-carbon-coordinating ligand, (hbz), ancillary ligand, not main ligand (mpz). The photophysical properties of the excited states of the Ir(mpz)$_2$hbz are investigated by comparing with the ligands (mpz and hbz) and dimmer emission, [Ir(mpz)$_2$Cl]$_2$. Finally, device performances of Ir(mpz)$_2$hbz doped polymer electrophosphorescent LEDs are also investigated. A mixture of PVN and PBD (60:40 by weight percent) or PVK is used as host matrics. The Ir(mpz)$_2$hbz doped PVN:PBD electrophosphorescent LEDs furnishes higher external quantum efficiency and luminance than those of Ir(mpz)$_2$hbz doped PVK electrophosphorescent LEDs.

Experimental

Figure 1 shows (a) device configuration and (b) chemical structures of hbz, [Ir(mpz)$_2$Cl]$_2$, Ir(mpz)$_2$hbz, PVK, PVN and PBD. The complex, Ir(mpz)$_2$hbz, was synthesized from the dimmer [Ir(mpz)$_2$Cl]$_2$ by refluxing 0.1 m mol of the dimmer and 2 m mol of hbz in 15 mL of methanol in the presence of 0.5 m mol of Na_2CO_3 for 8 h. The green residue was filtered and washed with water, ether and hexane and dried under vacuum. The compound was purified by using a column of silica and dichloromethane and acetone mixture (9:1) as the eluent. After rotary evaporation of the solvent, the compound was obtained as a yellowish green solid. The synthesis of the complex was confirmed from the elemental analyses and NMR spectra. Elemental analysis, Found: C% 56.42, H% 3.79. N% 9.86; Calculated: C% 56.57, H% 3.71. N% 10. ^{1}H NMR (300 MHz, $CDCl_3$) ppm 7.98 (d, 1H), 7.88 (t, 2H), 7.39 (d, 1H), 7.18 – 7.00 (m, 4H), 6.92 (d, 2H), 6.69 (t, 3H), 6.42 (d, 2H), 6.27 – 6.21 (m, 4H), 5.93 (d, 1H), 2.39 (s, 3H), 1.86 (s,3H). Element analyses were performed by using a Thermo Quest Italia S.p.A. EA1110 CHNS-O analyzer. ^{1}H NMR spectra were recorded at 300 MHz with a JEOL JNM-LA 300 WB FT-NMR spectrometer. The chemical shifts were referenced to internal SiMe4.

Absorption spectra were recorded on a Hewlett-Packard HP8452A UV-visible diode array spectrophotometer equipped with a Hewlett-Packard HP Vectra Qs 16 computer and corrected for background absorption. Photoluminescence spectra were detected by ACTON spectrometer connected to a photomultiplier tube (Acton Research PD-438) with Xenon lamp as excitation source.

Cyclic voltametry was performed with an Autolab potentiostat by Echochemie under nitrogen in a one-compartment electrolysis cell consisting of a platinum wire working electrode, a platinum wire counter electrode, and a quasi $Ag^+/AgCl$ reference electrode. The concentration of the complex was maintained at 0.5 mM or less and each solution contained 0.1 mM of tetrabutylammonium hexafluorophosphate (Aldrich) as the electrolyte. The oxidation of ferrocene in such a system takes place at 0.37 V. The HOMO level with reference to ferrocene gives the energy corresponding to vacuum level.

A mixture of PVN and PBD (60:40 by weight percent) or PVK was used as the host, respectively. The glass substrate pre-coated with indium-tin-oxide was cleaned by an ultrasonic bath of acetone, followed by 2-propanol. Surface treatment was

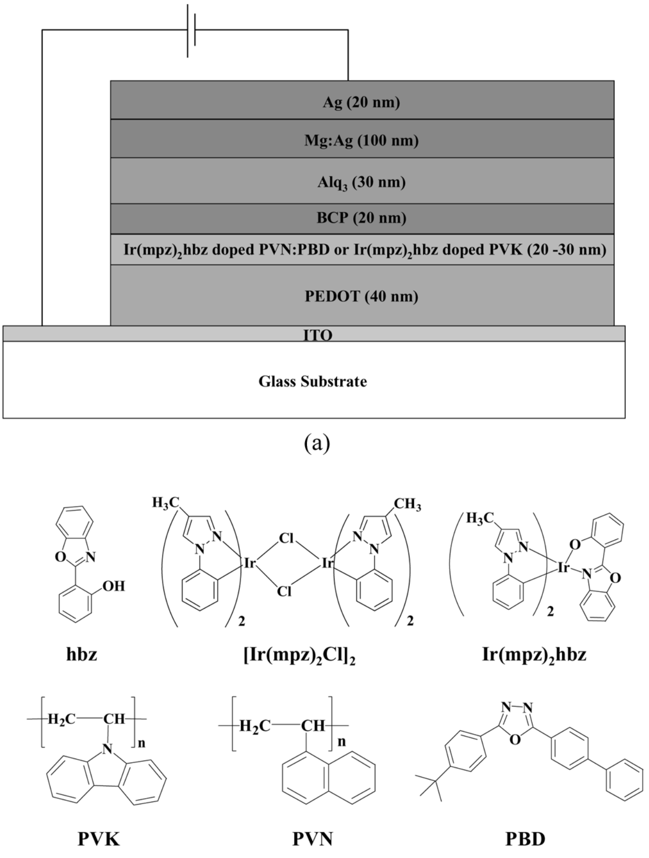

(a)

(b)

Figure 1. (a) Device configuration and (b) chemical structures of hbz, $[Ir(mpz)_2Cl]_2$, $Ir(mpz)_2hbz$, PVK, PVN and PBD.

carried out by exposing ITO to UV-ozone plasma. Electrophosphorescent polymer light emitting diodes which using PVN:PBD or PVK as host were fabricated as follows. The hole injecting poly(3,4-ethylene dioxythiophene) (PEDOT) layer was spin coated on the ITO with the thickness of 40 nm and baked at 120°C for 10 min in the oven. $Ir(mpz)_2hbz$ doped host layers (PVN:PBD or PVK) were spin coated on the PEDOT layer. The doping concentration was 8 wt%. A 20 nm thick BCP (2,9-dimethyl-4,7-diphenyl-1,10-phenanthroline) layer was then deposited as the exciton-blocking and the electron transporting layer followed by a 30 nm Alq_3 (tris-(8-hydroxyquinoline)aluminum(III)) as an electron transporting layer. Finally, a Mg-Ag layer (100 nm) capped by 20 nm of Ag were deposited as the cathode through a shadow mask by thermal evaporation. The fabricated multilayer polymer light emitting devices have two structures of ITO/PEDOT (40 nm)/PVN:PBD-$Ir(mpz)_2hbz$ (20–30 nm)/BCP (20 nm)/Alq_3 (30 nm)/Mg:Ag (100 nm)/Ag (20 nm) or ITO/PEDOT (40 nm)/PVK-$Ir(mpz)_2hbz$ (20–30 nm)/BCP (20 nm)/Alq_3 (30 nm)/Mg:Ag (100 nm)/Ag (20 nm). Current-voltage-luminescence characteristics of the devices were obtained by using a Keithley 237 Source Measurement Unit and a calibrated silicon photodiode connected with an optical power meter (Newport 1835-C).

Results and Discussion

Room temperature absorption spectra of mpz, hbz, $[Ir(mpz)_2Cl]_2$ and $Ir(mpz)_2hbz$ are shown in Figure 2(a). The absorption features below 300 nm correspond to the ligand centered absorption in both $[Ir(mpz)_2Cl]_2$ and $Ir(mpz)_2hbz$. The bands above 300 nm in the $[Ir(mpz)_2Cl]_2$ and $Ir(mpz)_2hbz$ can be ascribed as the absorption from the ground state to the states, which are considered as the admixture of the MLCT and ligand centered states. A sharp peak at 231 nm and peaks at 410 and 430 nm in $Ir(mpz)_2hbz$ can be attributed to hbz-centered absorption and to the MLCT bands of hbz parentage by comparing $[Ir(mpz)_2Cl]_2$ with $Ir(mpz)_2hbz$. The absorption at 336 nm which assumes to be MLCT absorption in $[Ir(mpz)_2Cl]_2$ has almost disappeared in $Ir(mpz)_2hbz$. The MLCT absorption bands are better resolved in $Ir(mpz)_2hbz$.

The emission (PL) and excitation (PLE) spectra of $Ir(mpz)_2hbz$ and the emission spectrum of hbz are given in Figure 2(b). The PLE spectrum of $Ir(mpz)_2hbz$ shows

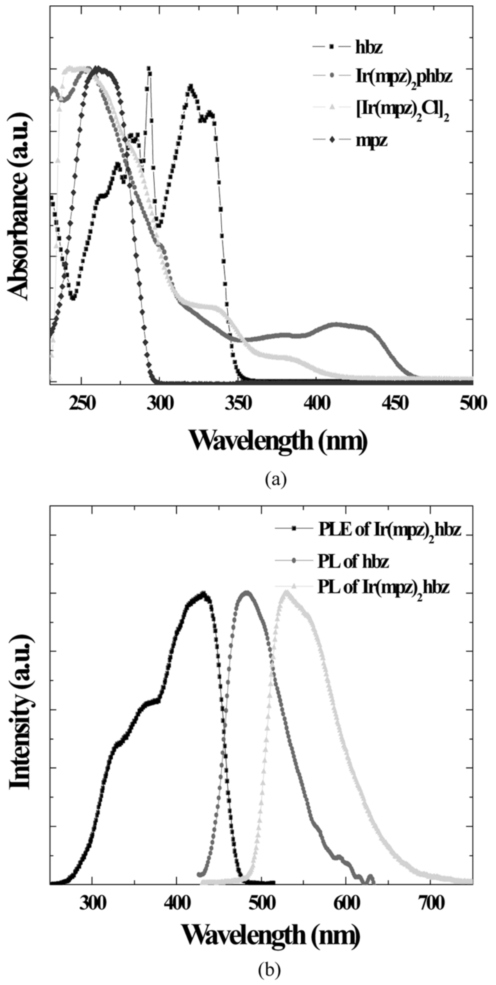

(a)

(b)

Figure 2. (a) Absorption spectra of 10^{-5} M solutions of mpz, hbz, $[Ir(mpz)_2Cl]_2$ and $Ir(mpz)_2hbz$ in dichloromethane at room temperature. (b) PLE spectra of $Ir(mpz)_2hbz$, PL spectra of hbz and $Ir(mpz)_2hbz$ in 10^{-5} M dichloromethane solution.

the similar features of the absorption spectrum. The hbz and Ir(mpz)$_2$hbz exhibit peak emissions at 482 and 530 nm, respectively, in dichloromethane solutions at room temperature. We have synthesized Ir(mpz)$_2$acac to observe the emission from the Ir(mpz)$_2$ unit. However, any noticeable emission is not observed. It is expected that Ir(mpz)$_2$hbz emission would result from hbz centered blue emission. The 50 nm red shifted emission in the Ir(mpz)$_2$hbz compare to hbz and new features in the absorption spectrum can be ascribed to the MLCT transitions based on hbz. The spectral shape of Ir(mpz)$_2$hbz remains the same when excited by either the ligand centered or MLCT centered transition. Maximum PL intensity is obtained at 430 nm excitation wavelength. From the incorporation with absorption spectrum, we assume that 430 nm is main ^{1}MLCT state. A substantial overlap of the hbz and

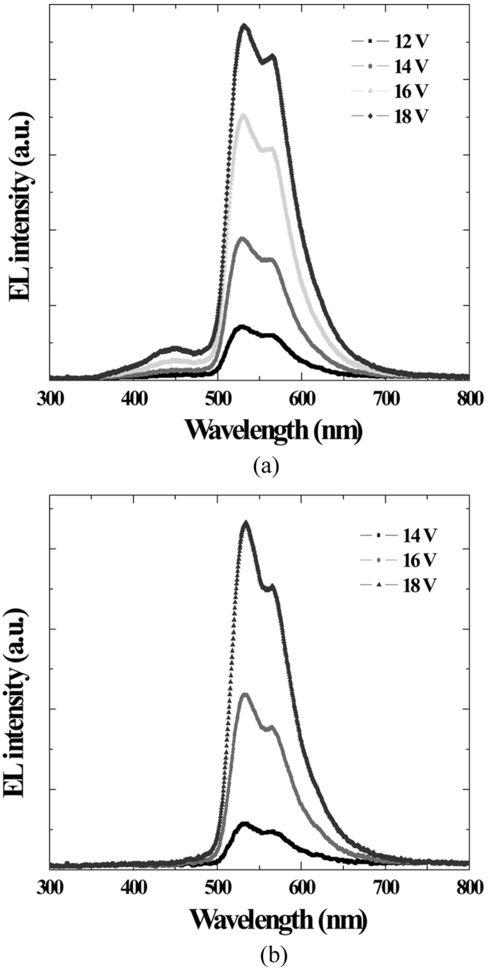

Figure 3. (a) EL spectra of 8 wt% Ir(mpz)$_2$hbz doped PVN:PBD device as function of applied voltage. Device configuration is ITO/PEDOT (40 nm)/PVN:PBD-Ir(mpz)$_2$hbz (20–30 nm)/BCP (20 nm)/Alq$_3$ (30 nm)/Mg:Ag (100 nm)/Ag (20 nm). (b) The EL spectral of 8 wt% Ir(mpz)$_2$hbz doped PVK device as function of applied voltage. Device configuration is ITO/PEDOT (40 nm)/PVK-Ir(mpz)$_2$hbz (20–30 nm)/BCP (20 nm)/Alq$_3$ (30 nm)/Mg:Ag (100 nm)/Ag (20 nm).

Ir(mpz)$_2$hbz emission predicts higher ligand characteristics in the MLCT state. A stokes shift of 4423 cm^{-1} between the MLCT absorption and emission also supports the higher ligand characteristics in the MLCT state.

The Ir(mpz)$_2$hbz shows reversible oxidation process in cyclic voltametric studies. The HOMO level is found to be 5.2 eV referenced to vacuum. The energy level of the singlet metal-to-ligand charge-transfer (^{1}MLCT) state is determined from the HOMO level and absorption at 430 nm; that of triplet metal-to-ligand charge-transfer (^{3}MLCT) is determined from HOMO and emission at 530 nm. Thus, the ^{1}MLCT and ^{3}MLCT states are assigned the values of 2.30 eV and 2.85 eV, respectively.

The EL spectra of (a) 8 wt% Ir(mpz)$_2$hbz doped PVN:PBD and (b) 8 wt% Ir(mpz)$_2$hbz doped PVK devices are shown in Figure 3. The EL spectra shapes are similar both in 8 wt% Ir(mpz)$_2$hbz doped PVN:PBD device and 8 wt% Ir(mpz)$_2$hbz doped PVK device. The peak luminance is observed at 530 nm with

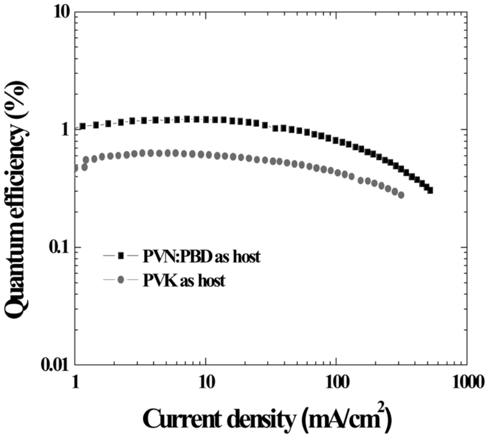

(a)

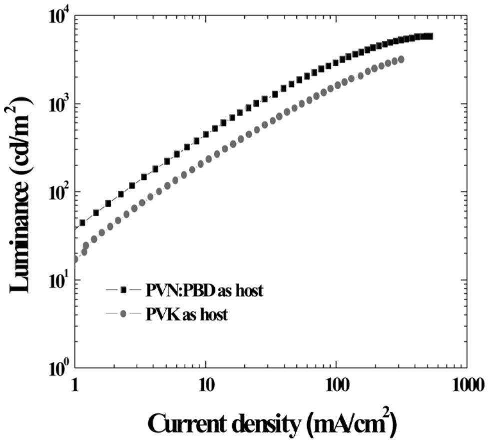

(b)

Figure 4. (a) The external quantum efficiency (η_{ext}) of 8 wt% Ir(mpz)$_2$hbz doped PVN:PBD device and 8 wt% Ir(mpz)$_2$hbz doped PVK device versus current density. (b) Luminance versus current density of 8 wt% Ir(mpz)$_2$hbz doped PVN:PBD device and 8 wt% Ir(mpz)$_2$hbz doped PVK device.

the sharper sub peak at 564 nm similar to solution PL spectra. These two peak emissions can be attributed to the vibronic progressions of the same electronic transition. The EL spectral shape remains unchanged at higher voltage. In Figure 3(a), a weak broad emission at ~450 nm is observed in 8 wt% $Ir(mpz)_2hbz$ doped the PVN:PBD device. The EL spectrum of ITO/PVN:PBD/Ca has a main peak at about 375 nm [3]. Two possibility would be assumed as reasons of the EL spectrum at ~450 nm. One is the EL spectrum of pristine PVN. The EL spectrum of PVN in the device of ITO/PVN/Ca is shown at 440 nm [3]. The other possibility is the emission from hole blocking BCP layer [4–5]. The CIE color coordinates are $x = 0.35$, $y = 0.56$ for 8 wt% $Ir(mpz)_2hbz$ doped PVN:PBD device and $x = 0.37$, $y = 0.57$ for 8 wt% $Ir(mpz)_2hbz$ doped PVK based device at the 14 V.

Figure 4 shows (a) external quantum efficiency (η_{ext}) and (b) luminance of 8 wt% $Ir(mpz)_2hbz$ doped PVN:PBD device and 8 wt% $Ir(mpz)_2hbz$ doped PVK device versus current density. The maximum quantum efficiency of 8 wt% $Ir(mpz)_2hbz$ doped PVN:PBD device is 1.2% at 12 mA/cm^2. The maximum brightness is 5,800 cd/m^2 at 18 V. An 8 wt% $Ir(mpz)_2hbz$ doped PVK device furnishes an external quantum efficiency of 0.6% at 6 mA/cm^2. The maximum brightness obtained is 3,100 cd/m^2 at 20 V. The $Ir(mpz)_2hbz$ doped PVN:PBD device demonstrates higher external quantum efficiency and luminance than those of $Ir(mpz)_2hbz$ doped PVK device. The higher quantum efficiency and luminance is originated from better balance of the electrons and holes in the mixed host device.

Conclusions

A new green emitting bis-orthometalated Ir(III) complex, $Ir(mpz)_2hbz$, has been synthesized and the photophysical properties as well as the device performances have been investigated by doping the complex in a mixture of PVN and PBD or PVK host. The $Ir(mpz)_2hbz$ emits the luminescence from the MLCT state, based on a non-carbon-coordinating ligand (hbz), but not from the orthometalated carbon-coordinating ligand (mpz). The 8 wt% $Ir(mpz)_2hbz$ doped PVN:PBD device demonstrates a better performance than that of 8 wt% $Ir(mpz)_2hbz$ doped the PVK device due to better hole and electron balance in the emissive layer. The maximum external quantum efficiency and luminance at 8 wt% $Ir(mpz)_2hbz$ doped PVN:PBD device is 1.2% and 5,800 cd/m^2. This work proves that MLCT transition based on a non-carbon bonding ligand can comply with the device demand.

Acknowledgments

This work was supported by Korea Ministry of Education, Science and Technology through the Global Partnership Program and APRI-Research Program through a grant provided by Gwangju Institute of Science and Technology.

References

[1] Colombo, M. G., Brunold, T. C., Riedener, T., Güdel, H. U., Förstch, M., & Bürgi, H.-B. (1994). *Inorg. Chem.*, *33*, 545.

[2] Lever, A. B. P. (1984). *Inorganic Electronic Spectroscopy* (Second Edition), Elsevier: New York.

[3] Jiang, X., Jen, A. K. Y., Carlson, B., & Dalton, L. R. (2002). *Appl. Phys. Lett.*, *81*, 3125.

[4] Lee, C.-L., Das, R. R., & Kim, J.-J. (2004). *Chem. Mater.*, *16*, 4642

[5] Lee, C.-L., Das, R. R., & Kim, J.-J. (2005). *Curr. Appl. Phys.*, *5*, 309.